

Electrically induced undulations and their competition with electrically induced convection in cholesteric liquid crystals

Harald Pleiner*

Department of Physics, University of Colorado, P.O. Box 390, Boulder, Colorado 80309-0390

Helmut R. Brand

*Department of Physics, University of Essen, D-4300 Essen, West Germany[†]
and Center for Nonlinear Studies (Mail Stop B258), Los Alamos National Laboratory, University of California,
Los Alamos, New Mexico 87545*

(Received 4 May 1987)

We show that cholesteric liquid crystals with a sufficiently short pitch, when put in an electric field, can exhibit undulations, the analog of mechanical undulations or of thermal undulations obtained when an external pressure or a temperature gradient is applied, respectively. As the pitch is increased a competition between the electric-field-induced undulations and the electrohydrodynamic instability arises. We give numerical estimates for both instabilities in this system, which represents another example of a competition between a constrained pattern-forming equilibrium system (electric-field-induced undulations) and a nonequilibrium (electrohydrodynamic) instability.

I. INTRODUCTION

We have recently shown¹ that in cholesteric liquid crystals subject to an external temperature gradient, a competition between two different types of instabilities arises. Depending on the size of the pitch, either a static instability (thermal undulations) or a hydrodynamic instability (thermal convection) occurs first.

Over the last few years the competition between instabilities has been discussed theoretically and experimentally for a number of systems, including onset of convection in binary-fluid mixtures,^{2,3} onset of convection in nematic liquid crystals⁴ and viscoelastic liquids,^{5,6} and the Taylor instability between independently rotating cylinders.^{7,8} In all these systems a codimension-2 point⁹ arises, for which the thresholds of the two instabilities are equal.

In contrast to all these examples, cholesteric liquid crystals seem to be the only system which can become unstable statically or dynamically due to the same external field. Here we point out that such a situation can occur in an external electric field (similar to the case of a temperature gradient, but in contrast to the case of an external magnetic field). The competition between instabilities emerges in the present case, since there is not only the well-known electrohydrodynamic instability,^{10,11} but also an electric-field-induced undulative instability possible, a fact which has not been reported so far.¹²

Such an interference of static and dynamic instabilities can also be studied by applying more than one external field, e.g., a temperature gradient and an external magnetic field in nematic liquid crystals.⁴

Layered structures, such as smectic and cholesteric liquid crystals (the "layers" of the latter are planes of equal phase of the helix formed by the director; the "layer thickness" is therefore the pitch¹¹) are known to undergo an undulative instability if dilated above a certain

threshold.^{13,14} Because of intrinsic nonlinearities in the elastic energy of these systems, it is then energetically more favorable to have the layers undulated (and less dilated) than flat (and more dilated). This mechanism works when the dilation is homogeneous (if the dilation is generated mechanically) or inhomogeneous (in the case of the temperature gradient or electric field), even if some regions are compressed rather than dilated. Of course, the threshold value for the onset of the instability depends on the spatial distribution of dilation.

An electric field generates dilation (or compression) due to two effects: (i) the balance of permeation and electric-field-induced permeation necessary for a stationary state, where electric-field-induced permeation describes the dissipative cross coupling between layer displacement and electric field¹⁵ (the analogous effect with respect to temperature gradients is the thermal permeation¹⁶), and (ii) the piezoelectric effect,¹⁵ i.e., the static cross coupling between (first) gradients of the displacement and the electric field. This effect is specific for cholesteric and chiral smectic liquid crystals and is not present in smectic-*A* liquid crystals. For both effects the electric field has to be along the helical axis.

If the electric field is strong enough, the induced dilation may then exceed the threshold for the undulation instability [electric-field-induced undulation (EU) instability]. For fixed boundaries at the top and at the bottom of the sample the piezoelectric effect will lead to the instability, while for a free top boundary only the electric-field-induced permeation effect contributes. Explicit formulas will be given in Sec. II.

On the other hand, it is well known that a cholesteric liquid crystal (like a nematic liquid crystal) can show an electrohydrodynamic instability (EHD), if subject to an external electric field.¹⁰ Such a hydrodynamic instability arises if the system becomes unstable against time-dependent fluctuations. Linear stability is tested by (linear) fluctuations with an exponential time behavior

$[\sim \exp(-\lambda t)]$ of all hydrodynamic variables: If at least the real part of one eigenvalue λ changes sign, the threshold for the instability is reached.

The most important part of the mechanism leading to EHD in cholesteric liquid crystals is connected with the anisotropy of the electric conductivity (Carr-Helfrich mechanism¹⁷⁻¹⁹). The elastic restoring force acting on layer fluctuations can be overcome by the electric force between space charges, which are created in the layer fluctuations due to the anisotropy of the electric conductivity. An explicit derivation of the threshold condition for EHD, which includes the coupling between helical structure and vorticity specific for cholesteric liquid crystals, will be given in Sec. III.

Since there are two different kinds of instabilities possible, a competition can arise. The instability whose threshold is lower will actually occur. Among the quantities which determine both thresholds are the sample thickness and the helical pitch, which can be varied over a very broad range. The magnitude of the pitch governs the rigidity of the layer structure, i.e., small (large) pitch mean large (small) bulk elastic modulus¹¹ (the stiffness against layer bending is independent of the pitch). Thus for small-pitch cholesteric liquid crystals even small dilations are energetically unfavorable and the threshold for the EU instability will be low. On the contrary, the elastic restoring force is large and can be overcome by a large electric force only, i.e., the threshold for the EHD instability is high. Of course, for large-pitch cholesteric liquid crystals the situation is reversed and there must be some crossover region at intermediate values of the pitch where the thresholds for the two different instabilities coincide. A more quantitative discussion of this region will be given in Sec. IV. Although the values of some of the material parameters involved are not known precisely (the instabilities might be used to measure them), we expect this crossover region to be accessible experimentally.

The threshold fields for the two instabilities depend on the sample thickness d in different manners: While for EHD it is a $d^{-1/2}$ law, for EU it is a d^{-2} or d^{-1} behavior (depending on whether the piezoelectric effect or electric-field-induced permeation is relevant). Thus electric-field-induced undulations will be favored by thick samples, while in thin samples the EHD instability is more likely to occur.

There are other restrictions for the occurrence of the instabilities. The EHD instability is possible only if the conductivity anisotropy is negative, while the EU instability is (in the relevant pitch region) independent of dielectric or conductivity anisotropy. On the other

hand, the EHD instability threshold is invariant under the reversal of the electric field, while EU instability can occur only with one specific sense of direction of the field, which one depends on the sign of a certain hydrodynamic parameter and the handedness of the helix. Again, this is a feature which should help to discriminate the two different types of instability.

In this paper we restrict ourselves to the onset of the instability, i.e., we do not address the question of which pattern is selected above threshold. Nevertheless, from the nature of the fluctuations, which become unstable at threshold, one can gain some hints about the structure above threshold. The spatial patterns to be expected above threshold for both kinds of instabilities seem to be similar to the extent that they include all hydrodynamic degrees of freedom, i.e., layer deformation, flow velocity,²⁰ electric current, etc., are all contributing to the spatial pattern.

II. ELECTRIC-FIELD-INDUCED UNDULATIVE INSTABILITY

We start with the discussion of the static coupling between the "layer" (helix) displacement u and the electric field \mathbf{E} . The free-energy density of these degrees of freedom is

$$\epsilon = \frac{B}{2} \gamma_{\parallel}^2 + \frac{K}{2} (\Delta_{\perp} u)^2 - \frac{1}{2} [\chi_{\perp} \mathbf{E}^2 + \chi_a (\mathbf{E} \cdot \hat{\mathbf{p}})^2] - \frac{1}{8\pi} \mathbf{E}^2 - \zeta^p q_0 (\hat{\mathbf{p}} \cdot \mathbf{E}) \gamma_{\parallel} - \zeta_{ijk}^F E_i \nabla_j \nabla_k u, \quad (2.1)$$

which contains the pure elastic and curvature terms,²¹ the pure electric terms,¹¹ and piezoelectric and flexoelectric terms,^{15,22} respectively. The dilation of the layers, γ_{\parallel} , is in lowest order of the appropriate gradients given by $\gamma_{\parallel} = \nabla_z u - \frac{1}{2} (\nabla_{\perp} u)^2$, where we have chosen the equilibrium direction of the helix to be the z axis. Fluctuations of the helix axis are described by gradients of u and to lowest order $\hat{\mathbf{p}} = \hat{\mathbf{p}}^0 [1 - \frac{1}{2} (\nabla_{\perp} u)^2] - \nabla_{\perp} u$, where $\hat{\mathbf{p}}^0 = \hat{\mathbf{e}}_z$ and $\hat{\mathbf{e}}_z \cdot \nabla_{\perp} \equiv 0$. The flexoelectric tensor ζ_{ijk}^F has the same structure as in smectic- A liquid crystals, while the piezoelectric term (ζ^p) is specific for systems without inversion symmetry, like cholesteric and chiral smectic liquid crystals.¹⁵

The polarization \mathbf{P} and the elastic restoring force $\text{div} \phi$ can easily be deduced from (2.1) by variational derivatives

$$\mathbf{P} = - \frac{\delta \epsilon}{\delta \mathbf{E}} - \frac{\mathbf{E}}{4\pi} \quad \text{and} \quad \phi = \frac{\delta \epsilon}{\delta \nabla u}. \quad (2.2)$$

The dynamical equations are^{15,16,21,23}

$$\left[\frac{\partial}{\partial t} + \mathbf{v} \cdot \nabla \right] u - \hat{\mathbf{p}} \cdot \mathbf{v} - \frac{1}{q_0} \hat{\mathbf{p}} \cdot \boldsymbol{\omega} - q_0 (g_a \hat{\mathbf{p}}_i \hat{\mathbf{p}}_j \nabla_j v_i + g_{\perp} \text{div} \mathbf{v}) = \zeta \text{div} \phi + \psi \hat{\mathbf{p}} \cdot \mathbf{E} \quad (2.3)$$

and

$$\left[\frac{\partial}{\partial t} + \mathbf{v} \cdot \nabla \right] \rho_{el} + \nabla \cdot [\sigma_a \hat{\mathbf{p}} (\hat{\mathbf{p}} \cdot \mathbf{E}) + \sigma_{\perp} \mathbf{E} + \psi \hat{\mathbf{p}} \text{div} \phi] = 0, \quad (2.4)$$

where \mathbf{v} is the velocity, $\boldsymbol{\omega} = \frac{1}{2} \text{curl} \mathbf{v}$ the vorticity, and ρ_{el} the electric charge density. The other hydrodynamic equations will not be needed here explicitly. The thermal degree of freedom is suppressed in (2.3) and (2.4).

Looking for a stationary ($\partial/\partial t = 0$), nonconvective ($\mathbf{v} = 0$) equilibrium state in the presence of an external, homogeneous field \mathbf{E}_{ext} along the helix axis $\hat{\mathbf{p}}^0$, only the dissipative terms in (2.3) and (2.4) survive: permeation (ζ), electric-field-induced permeation (ψ), and electric conductivity (σ_{\perp}, σ_a). The desired solution is

$$\text{div} \boldsymbol{\phi} = -\frac{\psi}{\zeta} \mathbf{E}_{\text{ext}} = \text{const} \quad (2.5)$$

and

$$\hat{\mathbf{p}} = \hat{\mathbf{p}}^0 = \hat{\mathbf{e}}_z,$$

which gives rise to an equilibrium polarization

$$\mathbf{P} = \hat{\mathbf{e}}_z \left[\tilde{\chi}_{\parallel} - z q_0 \zeta^p \frac{\psi}{\zeta B} \right] \mathbf{E}_{\text{ext}} \quad (2.6)$$

and an equilibrium layer dilation (or compression)

$$\frac{du}{dz} = \left[-\frac{\psi}{\zeta B} z + c_0 \right] \mathbf{E}_{\text{ext}}, \quad (2.7)$$

where the constant c_0 depends on the boundary conditions and where $\tilde{\chi}_{\parallel} = \chi_{\parallel} + \zeta^p q_0 c_0 - \zeta^F \psi / \zeta B$ is a renormalized electric susceptibility. For a layer with fixed plates at the bottom ($z=0$) and the top ($z=d$), $c_0 = d \psi (2 \zeta B)^{-1}$, while if the top is a free boundary, $\phi_z(z=d) = 0$ and $c_0 = (d \psi \zeta^{-1} + \zeta^p q_0) B^{-1}$.

It is easy to check that with the solution (2.5)–(2.7) the continuity, the Navier-Stokes, and the energy conservation equations are solved identically; the temperature and the mass density are constant, while the pressure is a linear function of z .

The nonvanishing equilibrium polarization \mathbf{P} gives rise to an electric surface charge density $4\pi \tilde{\chi}_{\parallel} \mathbf{E}_{\text{ext}}$. These charges produce an electric field (although partially screened), which acts opposite to the external field. Thus the local field E_0 is smaller than the external field E_{ext} and in Eqs. (2.5)–(2.7) E_{ext} has to be replaced by $E_0 = E_{\text{ext}} / (1 + 4\pi \tilde{\chi}_{\parallel})$. There is also a small bulk charge density, $\text{div} \mathbf{P} \neq 0$, whose field we neglect against E_{ext} or E_0 , because $\text{div} \mathbf{P}$ is quadratic in the small off-diagonal terms $\zeta^p q_0$ and $\psi / \zeta B$. In the same spirit $\tilde{\chi}_{\parallel}$ is replaced by χ_{\parallel} .

The layer displacement u caused by the external electric field now constitutes dilation ($du/dz > 0$) at least in parts of the sample, depending on the signs of ψ , ζ^p , or E_0 . It is then straightforward to test the stability of this dilation against undulative fluctuations.¹³ Assuming

$$u = \left[-\frac{1}{2} z^2 \frac{\psi}{\zeta B} + c_0 z \right] E_0 + A \cos(k_{\perp} x) \sin(k_z z), \quad (2.8)$$

with $k_z = \pi / 2 \eta d$, where $\eta = \frac{1}{2}$ and 1 for fixed and free top boundaries, respectively, and with the local field E_0 remaining constant,²⁴ the total energy $E = \int \epsilon dV$ can

be calculated as a function of the amplitude A . It turns out that E is a minimum for $A = 0$ only below a certain threshold field E_0^{th} , above which the state $A = 0$ becomes unstable. This threshold field is given by

$$E_0^{\text{th}} = \frac{1}{c_1} k_z (BK)^{1/2}, \quad (2.9)$$

where $c_1 = (\eta - \frac{1}{2}) \psi d (\pi^2 - 4) / 2\pi^2 \zeta + (\eta - 1) \zeta^p q_0$. The critical transverse wave vector is

$$k_{\perp}^{\text{th}} = k_z^{1/2} \left[\frac{B}{K} \right]^{1/4}, \quad (2.10)$$

with the appropriate length scale $L_{\perp} \sim (dL_p)^{1/2}$ smaller than the sample thickness d as long as the pitch length L_p is smaller than d (which is assumed throughout this paper).

Since the signs of ζ^p and ψ (and thus of c_1) are not fixed, the direction of \mathbf{E}_{ext} has to be chosen in order to get $E_0 c_1$ positive. For a fixed top boundary ($\eta = \frac{1}{2}$) the electric-field-induced permeation effect drops out and the piezoelectric effect is solely responsible for the instability ($E_0^{\text{th}} \sim 1/\zeta^p$). This can be understood quite generally: any energy contribution not connected with the handedness must be invariant under $E_{\text{ext}} \rightarrow -E_{\text{ext}}$, if dilation and compression are symmetrically distributed in either half of the sample (as it is indeed the case for $\eta = \frac{1}{2}$). Since the threshold is linear in the electric field, this symmetry would rule out any finite threshold field E_0^{th} . However, the piezoelectric energy does depend on the handedness of the helix and is different for E_{ext} and $-E_{\text{ext}}$, even if dilation and compression are symmetric. An instability is possible only if $E_0 \zeta^p < 0$.

For free top boundaries ($\eta = 1$) there is an instability, if \mathbf{E}_{ext} is chosen, so that $E_0 \psi > 0$. In this case the piezoelectric effect drops out and electric-field-induced permeation triggers the instability alone. It is quite characteristic for a free boundary that only dissipative terms can lead to an instability, since by adjusting the height of the sample, the static cross coupling contributions to the generalized energy always make the energy a minimum.

Apparently, the height d of the sample in the electric field is larger than the height d_0 without the dilation introduced by the electric field [$d/d_0 = 1 + (\zeta^p q_0 + d \psi / 2 \zeta) E_0 / B$].

Such a behavior was already obtained in the case of thermal undulations,¹ where with a free top boundary only the dissipative effect triggered the instability, but not the static one. On the other hand, for thermal undulations,¹ there was no instability found in the case of rigid boundaries, because no term with handedness (like the piezoelectric term) was introduced. However, there exists an analogous term in the free energy for cholesteric liquid crystals $\sim \zeta^T q_0 \nabla_z T \gamma_{\parallel}$, relating gradients of the temperature to compression or dilation of the layers. Usually that term is neglected in the thermal case against $\sim \gamma_2 \delta T \gamma_{\parallel}$, the thermal layer expansion effect.²⁵ (In the electric case, no such γ_2 effect exists). If ζ^T would have been kept in Ref. 1, an instability also in the case of fixed boundaries would have been found, with a

threshold given by Eq. (2.9) ($\nabla_z T$, ζ^T instead of E_0 , ζ^P , and $\eta = \frac{1}{2}$). In smectic- A liquid crystal systems, however, where terms with handedness are absent by symmetry, no electric-field-induced undulation instability can occur in the case of rigid boundaries.

In deriving (2.9) we have neglected the fact that an undulative fluctuation (2.8) also constitutes a local fluctuation of the helix axis, where $\hat{\mathbf{p}}$ is no longer parallel to \mathbf{E}_{ext} . For negative electric susceptibility anisotropy (with respect to $\hat{\mathbf{p}}$, not $\hat{\mathbf{n}}$), $\chi_a < 0$, this is a destabilizing effect which can lower the threshold. When including this susceptibility anisotropy effect, Eq. (2.9) reads

$$-\frac{1}{2}\chi_a(E_0^{\text{th}})^2 + c_1 E_0^{\text{th}} = k_z(BK)^{1/2}. \quad (2.11)$$

For $c_1 = 0$, the threshold field E_0^{th} is just that for the well-known electrical Helfrich-Hurault instability,¹⁰ a static instability against inhomogeneous tilt of the helix axis with respect to \mathbf{E}_{ext} .²⁶ Since this contribution to the threshold condition is quadratic in E_0 , a positive χ_a is always stabilizing and enhances the threshold. From our numerical estimates in Sec. IV, we conclude that—at least in the parameter range, where the undulation instability is the relevant one—the susceptibility anisotropy effect is only a small correction to the electric-field-induced permeation or piezoelectric effect, i.e., Eq. (2.9) can be used instead of (2.11).

III. ELECTROHYDRODYNAMIC INSTABILITY

The derivation of the threshold field for the EHD in cholesteric liquid crystals follows the general line for EHD in nematic liquid crystals. Since for the latter there exists a comprehensive literature,^{10–12,25,27} we can be brief here. The nonconvective, stationary state due to an external constant electric field (as discussed in Sec. II) is now probed for stability against time- $[\sim \exp(-\lambda t)]$ and space-dependent $[\exp(ik_1 x + ik_2 z)]$ infinitesimal fluctuations. The longitudinal wave vector is again chosen to accommodate boundary conditions, $k_z = \pi/2\eta d$ with $\eta = \frac{1}{2}$ and 1 for rigid and free top boundaries, respectively, while k_1 is obtained by minimizing the threshold.

As usual we will make the approximation of incompressibility ($\text{div } \mathbf{v} = 0$) and neglect longitudinal fluctuations of the electric field against the imposed field ($E_z = E_0$), and we will suppress the thermal degree of freedom. The dynamical equations are then given by (2.3), (2.4), and^{16,21,23}

$$\rho_{\text{mass}} \left[\frac{\partial}{\partial t} + \mathbf{v} \cdot \nabla \right] \mathbf{v} + \nabla p - \hat{\mathbf{p}} \text{div} \phi + \frac{1}{2q_0} (\hat{\mathbf{p}} \times \nabla) \text{div} \phi, \quad (3.1)$$

$$-g_a q_0 \hat{\mathbf{p}} (\hat{\mathbf{p}} \cdot \nabla) \text{div} \phi - \frac{1}{4\pi} \nabla \cdot (\mathbf{E} + 4\pi \mathbf{P}) \mathbf{E} = \mathbf{v} : \nabla \nabla \mathbf{v}.$$

The standard procedure of linear stability then gives the threshold value for E_0 , where λ changes sign. We find (neglecting electric-field-induced permeation, piezoelectricity, and flexoelectricity for the moment)

$$(E_0^{\text{th}})^2 = -\frac{Bk_z^2 + Kk_1^4}{k_1^2} (1 + l^2 k^2) \frac{4\pi\sigma_\perp}{\epsilon_z \sigma_a + \epsilon_a \sigma_z l^2 k^2}, \quad (3.2)$$

where

$$l^2 = \left[v_3 + v_1 \frac{k_z^2}{k_1^2} \right] \left[\xi + \frac{1}{4\pi q_0^2} \left[v_2 + v_3 \frac{k_z^2}{k_1^2} \right]^{-1} \right].$$

The viscosities v_α are according to the notation in Refs. 16, 28, and 29. It should be noted that even if permeation is neglected additionally ($\xi = 0$, as in Ref. 10), the longitudinal velocity v_z and the vorticity ω_z are not zero (and cannot be put to zero *a priori*), because of the intricate connection of vorticity and displacement in cholesteric liquid crystals (2.3). The $l^2 k^2$ term in (3.2) is partly due to this connection. However, the length l scales with the pitch length L_p and it turns out that $l^2 k^2 < 1$ as long as $L_p < d$. Neglecting $l^2 k^2$ in (3.2), the transverse wave vector, which minimizes E_0^{th} , is then found to be equal to that for the electric-field-induced undulative instability (2.10)

$$(k_1^{\text{th}})^2 = \frac{\pi}{2\eta d} \left[\frac{B}{K} \right]^{1/2} \sim (dL_p)^{-1} \quad (3.3)$$

and the threshold field is given by¹⁰

$$(E_0^{\text{th}})^2 = 2k_z(BK)^{1/2} \left[-\frac{4\sigma_\perp \pi}{\epsilon_z \sigma_a} \right]. \quad (3.4)$$

If electric-field-induced permeation and piezoelectricity (and flexoelectricity) are taken into account, the EHD instability is no longer a stationary one, but an oscillatory one (just as it is the case for thermal convection, if thermal permeation, etc., are taken into account³⁰). The frequency is proportional to ψ (and g_a , ζ^F) and thus probably very small. The threshold condition (3.4) is also changed and follows from a quadratic equation of the form

$$-\frac{\epsilon_z \sigma_a}{8\pi\sigma_\perp} (E_0^{\text{th}})^2 + c_2 E_0^{\text{th}} = k_z(BK)^{1/2}. \quad (3.5)$$

Our numerical estimates in Sec. IV suggest, however, that—in the relevant parameter range, where EHD occurs—the linear term $\sim E_0^{\text{th}}$ is less important in (3.5) than the quadratic term ($\sim E_0^{\text{th}2}$ and Eqs. (3.2) or (3.4) are a good approximation for the threshold field. Thus the EHD instability is not affected by field reversal and can only occur if σ_a is negative.

IV. NUMERICAL ESTIMATES AND COMPARISON

To compare the threshold fields for EU and EHD instability, one has to know the parameters entering (2.11) and (3.5). Unfortunately the electric-field-induced permeation and piezoelectric coefficients, ψ and ζ^P , are not known experimentally. It will rather be the other way around; measuring the crossover threshold field (see below) provides a method for obtaining experimental values of ψ and ζ^P . Since there are also no easy and reli-

able theoretical methods to calculate such coefficients, we can only give some estimates. There are upper bounds for off-diagonal elements of generalized thermodynamic potentials and of the entropy production matrix, because of static and thermodynamic stability, respectively. These Cauchy-Schwarz inequalities read [cf. (2.1), (2.3), and (2.4)]

$$\psi^2 \leq \xi \sigma_z, \quad (4.1)$$

and

$$(q_0 \xi^P)^2 \leq B(1 + 4\pi\chi_{\parallel}). \quad (4.2)$$

In cholesteric liquid crystals the elastic coefficient B is known to be roughly equal to KL_p^{-2} , while the permeation coefficient $\xi = \xi_{\text{nema}} L_p^2$, where ξ_{nema} is the orientational viscosity of nematics (sometimes called γ_1^{-1}). The pitch length L_p is related to the helical wave length by $|q_0| = 2\pi/L_p$. If one would use the equality sign in Eq. (4.1), ψ would be $\sim q_0^{-1}$. However, since q_0 is a pseudoscalar quantity ($q_0 \equiv \langle \hat{n} \cdot \text{curl} \hat{n} \rangle_{\text{eq}}$), odd powers of q_0 are already built in explicitly in the dynamical equations where necessary and it is expected that all coefficients are only functions of even powers of q_0 .³¹ To be consistent with the inequality (4.1) even for $L_p \rightarrow \infty$ (the nematic limit), $\psi = \text{const}$ is the appropriate choice. Of course, Eq. (4.1) is then violated for $L_p \rightarrow 0$. However, L_p cannot be smaller than some molecular length (e.g., length of the molecules), since then the notion of helix, etc., has already lost any meaning. Choosing ψ independent of L_p and so small that it does not violate (4.1) for all possible L_p , one gets (with $\sigma_z = 10^4 \text{ sec}^{-1}$, $\xi_{\text{nema}} = 10 \text{ cm sec/g}$) $\psi = \pm 2 \times 10^{-7} \text{ cm}^{3/2} \text{ g}^{-1/2}$. Even for a pitch as small as $L_p = 0.1 \mu\text{m}$, ψ is then two orders of magnitude smaller than the maximal allowed value by (4.1). For ξ^P we chose a value, which is—for all possible values of L_p —at least one order of magnitude smaller than allowed by (4.2) and find (with $K = 5 \times 10^{-7} \text{ g cm/sec}^2$, $\chi_{\parallel} = \frac{1}{3}$) $\xi^P = \pm 6 \times 10^{-6} \text{ g}^{1/2} \text{ cm}^{1/2} \text{ sec}^{-1}$. Of course, these values of ψ and ξ^P are rather guesses than estimates and all quantitative results obtained with these values must be taken with caution; the qualitative picture we will derive below, however, is not affected by these uncertainties.

The threshold conditions for EU and EHD instability, Eqs. (2.11) and (3.5), both have the form $-\frac{1}{2}\alpha_i (E_0^{\text{th}})^2 + c_i E_0^{\text{th}} = k_z (BK)^{1/2}$, where α_i ($\alpha_i = \chi_a$ or $\epsilon_z \sigma_a / \sigma_1 4\pi$ neglecting $l^2 k^2$ against 1) is independent of L_p or d , while $k_z (BK)^{1/2} \sim (dL_p)^{-1}$. The linear coefficients c_i contain two different types of terms, $d\psi/\xi$ and $q_0 \xi^P$ and which are $\sim d/L_p^2$ and $\sim L_p^{-1}$, respectively. Thus for large L_p (and small d) the term linear in E_0^{th} will become negligible against the quadratic term. In that case $(E_0^{\text{th}})^2 = -\alpha_i^{-1} 2k_z (BK)^{1/2}$ and the threshold for EHD is lower than that for EU, since usually $|\epsilon_z \sigma_a / \sigma_1|$ is larger than $|\epsilon_a|$. On the contrary, for small L_p (and large d) the quadratic term is less important and the threshold field is given by

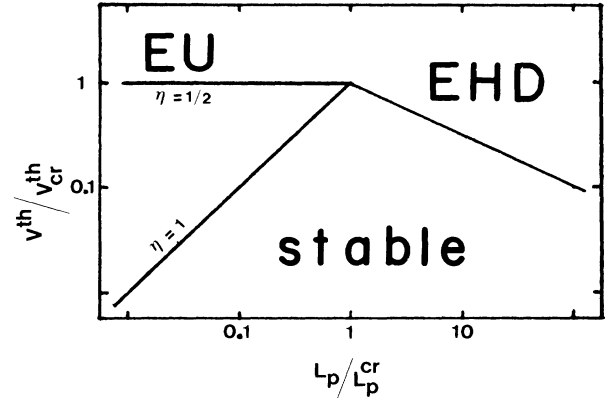


FIG. 1. Threshold voltages V^{th} as a function of the pitch length L_p (at constant sample thickness d) in double logarithmic plot; $\eta = \frac{1}{2}$ and 1 for fixed and free top boundaries, respectively; crossover values $V_{\text{cr}}^{\text{th}}$ and L_p^{cr} are discussed in text.

$E_0^{\text{th}} = c_i^{-1} k_z (BK)^{1/2}$. Now, the threshold for EU is lower than that for EHD, since $|c_1|$ is larger than $|c_2|$. Thus, there is a crossover pitch length L_p^{cr} (and a crossover sample thickness d_{cr}) which separates the EHD instability from the EU instability, whose threshold fields are given by (3.2) and (2.9), respectively. L_p^{cr} and d_{cr} are not independent of each other, but related linearly,

$$L_p^{\text{cr}} = \beta d_{\text{cr}}, \quad (4.3)$$

where the proportionality coefficient

$$\beta = (\psi^2 \sigma_1 / K \xi_{\text{nema}}^2 \epsilon_z |\sigma_a|)^{1/3} (1 - 4/\pi^2)^{2/3}$$

and

$$= 8\pi^2 \xi^2 \sigma_1 / K \epsilon_z |\sigma_a|$$

for $\eta = 1$ and $\frac{1}{2}$, respectively. With our numerical estimates $\beta \approx 4 \times 10^{-4}$ for both cases. The crossover threshold field, where the thresholds for EU and EHD instability are equal, is

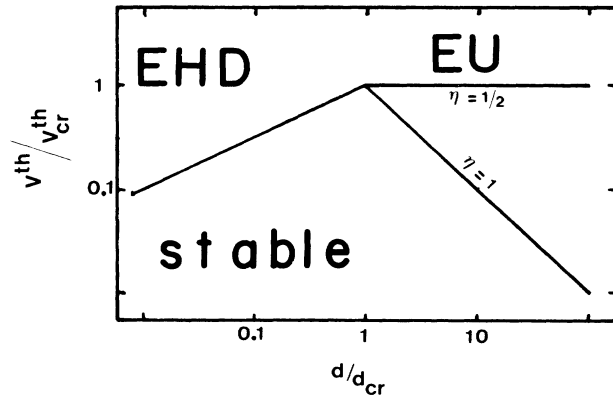


FIG. 2. Threshold voltages V^{th} as a function of the sample thickness d (at constant pitch length L_p) in double logarithmic plot; $\eta = \frac{1}{2}$ and 1 for fixed and free top boundaries, respectively; crossover values $V_{\text{cr}}^{\text{th}}$ and d_{cr} are discussed in text.

$$\begin{aligned}
 |E_{cr}^{th}| &= \frac{k_z(BK)^{1/2}}{|c_1|} = \left[\frac{k_z(BK)^{1/2}}{\frac{1}{2}|\alpha_2|} \right]^{1/2} \\
 &= \left[\frac{\pi K}{\eta\beta d_{cr}^2 |\alpha_2|} \right]^{1/2} \quad (4.4)
 \end{aligned}$$

Choosing a convenient crossover pitch length $L_p^{cr} = 1 \mu\text{m}$ (and thus $d_{cr} = \frac{1}{4}$ cm) the crossover field is ($\alpha_2 \approx 1$) $|E_{cr}^{th}| = 75$ and 60 V/cm (crossover voltage 20 and 15 V) for free ($\eta = 1$) and fixed ($\eta = \frac{1}{2}$) top boundaries. A schematic plot of the threshold voltages is given in Figs. 1 and 2.³²⁻³⁴

In conclusion, our crude estimates for ζ^p and ψ show

that the crossover can be reached experimentally in cholesteric liquid crystals, and by varying either the sample thickness or the pitch length one should proceed from a dynamical instability (EHD) to a static one (EU), and vice versa. As already stated in the Introduction, above threshold, however, the two kinds of instability might be rather similar in appearance.

ACKNOWLEDGMENTS

We thank the Deutsche Forschungsgemeinschaft for support of this work. The work of one of us (H.R.B.) at the Center for Nonlinear Studies (CNLS), Los Alamos National Laboratory (LANL), has also been supported by the U.S. Department of Energy (DOE).

*Present address: Institute for Theoretical Physics, University of California, Santa Barbara CA 93106.

†Permanent address.

¹H. Pleiner and H. R. Brand, Phys. Rev. A **32**, 3842 (1985).

²H. R. Brand, P. C. Hohenberg, and V. Steinberg, Phys. Rev. A **27**, 591 (1983); **30**, 2548 (1984).

³I. Rehberg and G. Ahlers, Phys. Rev. Lett. **55**, 500 (1985).

⁴E. Dubois-Violette and H. R. Brand (unpublished).

⁵B. J. A. Zielinska, D. Mukamel, and V. Steinberg, Phys. Rev. A **33**, 1454 (1986).

⁶H. R. Brand and B. J. A. Zielinska, Phys. Rev. Lett. **57**, 2768 (1986).

⁷C. D. Andereck, S. S. Liu, and H. L. Swinney, J. Fluid Mech. **164**, 155 (1986).

⁸C. D. Andereck, R. Dickman, and H. L. Swinney, Phys. Fluids **26**, 1395 (1987).

⁹J. Guckenheimer and P. Holmes, *Nonlinear Oscillations, Dynamical Systems, and Bifurcations of Vector Fields* (Springer, New York, 1983).

¹⁰S. Chandrasekhar, *Liquid Crystals* (Cambridge University Press, Cambridge, England, 1977).

¹¹P.-G. de Gennes, *The Physics of Liquid Crystals*, 3rd ed. (Clarendon, Oxford, 1982).

¹²L. M. Blinov, *Electro-Optical and Magneto-Optical Properties of Liquid Crystals* (Wiley, New York, 1983).

¹³N. A. Clark and R. B. Meyer, Appl. Phys. Lett. **22**, 493 (1973).

¹⁴M. Delaye, R. Ribotta, and G. Durand, Phys. Lett. **44A**, 139 (1973).

¹⁵H. R. Brand and H. Pleiner, J. Phys. (Paris) **45**, 563 (1984).

¹⁶P. C. Martin, O. Parodi, and P. S. Pershan, Phys. Rev. A **6**, 2401 (1972).

¹⁷E. F. Carr, Mol. Cryst. Liq. Cryst. **7**, 253 (1969).

¹⁸W. Helfrich, Mol. Cryst. Liq. Cryst. **21**, 187 (1973).

¹⁹For the case of an external temperature gradient, it is the anisotropy of the heat conduction which is important.

²⁰As in the case of the mechanically induced undulation instability, the undulative fluctuations leading to EU are not solu-

tions of the complete hydrodynamic equations as soon as they assume finite strength. Therefore flow is expected above threshold.

²¹T. C. Lubensky, Phys. Rev. A **6**, 452 (1972).

²²P.-G. de Gennes, J. Phys. C **30**, 65 (1969).

²³H. Brand and H. Pleiner, J. Phys. (Paris) Colloq. **41**, C-553 (1980).

²⁴The undulations $A \neq 0$ also produce a spatially nonuniform polarization, which in turn gives rise to an additional field. This field is, however, very small and is neglected against the (constant) local field E_0 .

²⁵Since the electric Helfrich-Hurault instability always has a lower threshold than the conical instability and the helix unwinding instability,¹⁰ the latter instabilities need not be considered here further.

²⁶E. Dubois-Violette, E. Guyon, and P. Pieranski, Mol. Cryst. Liq. Cryst. **26**, 193 (1975).

²⁷H. N. W. Lekkerkerker, J. Phys. (Paris) Lett. **38**, L277 (1977).

²⁸D. Forster, Ann. Phys. (N.Y.) **84**, 505 (1974).

²⁹Again, vector and tensor components are taken with respect to $\hat{p}^0 = \hat{e}_z$ as preferred direction, not with respect to the molecular axis (the director \hat{n}). For second rank tensors the relations between these two sets of components in cholesteric liquid crystals are $\tau_{\parallel}^n = \tau_z$, $\tau_{\parallel}^m = 2\tau_{\parallel} - \tau_z$, and $\tau_a^m = -2\tau_a$.

³⁰H. Pleiner and H. Brand, Phys. Rev. A **23**, 944 (1981).

³¹Of course, there could be a dependence on $|q_0|$ or any other nonanalytical function of q_0 —a possibility we will not consider further.

³²For ordinary smectic-*A* liquid crystals (with a layer thickness of $\approx 30 \text{ \AA}$) the crossover region cannot be reached. For the newly found smectic-*A* liquid crystals with giant layer spacing in the μ range (Ref. 33), however, the crossover from an undulative to a hydrodynamic instability seems to be a possibility—for the thermal as well as the electric case (free top boundary) (Ref. 34).

³³F. C. Larche, J. Appell, G. Porte, P. Bassereau, and J. Marignan, Phys. Rev. Lett. **56**, 1700 (1986).

³⁴H. R. Brand and H. Pleiner (unpublished).